

## Effects of Tissue Relaxation, Eddy currents, and Acceleration on Velocity-Selective Preparation Pulses

Taehoon Shin<sup>1,2\*</sup>

<sup>1</sup>Division of Mechanical and Biomedical Engineering, Ewha Womans University, Seoul, Republic of Korea

<sup>2</sup>Graduate Program in Smart Factory, Ewha Womans University, Seoul, Republic of Korea

(Received 7 October 2022, Received in final form 22 December 2022, Accepted 3 January 2023)

Fourier-transform-based velocity-selective (FT-VS) magnetization preparation has shown great promise for unenhanced MR angiography and arterial spin labeling. Although recent technical advances made FT-VS preparation resistant to  $B_0$  and  $B_1$  field inhomogeneity, there remain other non-ideal conditions including tissue relaxation, eddy currents, and accelerated motion, which are often ignored during excitation pulse design. In this study, using a double-refocused VS preparation pulse as a testbed, excitation profiles were numerically simulated taking into account the potential effects of the three non-ideal conditions. The longitudinal magnetization of arterial blood resulting from FT-VS preparation turned out to decrease from the ideal value of  $M_0$  to  $0.92M_0$ ,  $0.99M_0$ , and  $0.88M_0$  due to tissue relaxation, eddy currents, and accelerated motion, respectively. When all three factors were considered simultaneously, the worst-case relative contrast ratio (CR) between arterial blood and muscle tissue was estimated as 0.86, corresponding to a decrease by 14 % from the ideal CR of 1.0.

**Keywords :** velocity selective magnetization preparation, eddy currents, non-contrast-enhanced MR angiography

### 1. Introduction

Selective excitation of magnetic spins as a function of spin properties is an important step in magnetic resonance imaging (MRI) for enhancing image contrast. Spatially selective excitation is dominantly used for creating an electromagnetic signal only within an imaging volume of interest, and frequency-selective excitation is routinely used in magnetization preparation for suppressing signals from fat tissue. Fourier-transform-based velocity-selective (FT-VS) excitation is a relatively new type of excitation used for generating image contrast based on spin motion [1]. By exciting magnetic spins selectively based on their velocities, FT-VS excitation can generate image contrast between a moving tissue (*e.g.*, arterial blood) and a stationary tissue.

Among many possible VS excitation profiles, a notch-shaped longitudinal magnetization ( $M_z$ ) profile over velocity has been shown to be particularly useful for *in-vivo* applications (refer to Fig. 1B) [2]. When used for magnetization preparation, this type of VS excitation can

highlight fast moving arterial blood while suppressing signals originating from stationary tissues, and was first applied in non-contrast-enhanced MR angiography where all tissues but arteries need to be suppressed [3-5]. VS magnetization-prepared angiography has the advantages of high 3D spatial resolution as opposed to inflow-based 2D approaches, and acquisition of only a single image as opposed to subtractive 3D approaches [6]. VS angiography has been shown to be feasible for peripheral, cerebral, abdominal, and pedal arteries [7-10]. More recently, notch-shaped VS magnetization preparation has also been used for arterial spin labeling (ASL) applications [11-13]. An arterial blood-labeled image can be obtained by inverting stationary tissues but not arterial blood using a VS preparation, and it can be subtracted from the reference image to generate a quantitative perfusion map. Compared to the traditional VS-ASL, where the blood is labeled by saturation, the inversion-based labeling enhances signal-to-noise-ratio (SNR) by 20 % to 40 % [14, 15].

The primary issue in VS preparation had been its sensitivity to  $B_0$  and  $B_1$  field errors due to the use of multiple interleaved  $B_1$  and bipolar gradient pulses. The first design of VS excitation pulse was short and straightforward to implement but highly sensitive to  $B_0$

©The Korean Magnetism Society. All rights reserved.

\*Corresponding author: Tel: +82-2-3277-6534

Fax: +82-2-3277-3535, e-mail: shinage@gmail.com

field error (*i.e.*, off-resonance), resulting in a non-uniform background suppression [3]. The off-resonance sensitivity was greatly reduced by the addition of  $180^\circ$  refocusing pulses between the two unipolar gradients split from the original bipolar gradient [4]. However, this single-refocused design increased the sensitivity to  $B_1$  field error which reduced the accuracy of the refocusing and therefore caused signal loss in arterial blood [16]. The latest VS excitation pulse design employed two or four refocusing pulses within each velocity encoding step combined with Malcolm-Levitt (MLEV) phase cycling [17-19], and significantly improved the immunity to both  $B_0$  and  $B_1$  field errors. Artifactual stripes are another type of image artifacts which can occur when the  $180^\circ$  rotation of a refocusing pulse is not perfect. Based on characterization of the stripes using phase graph analysis, we previously proposed alternately applying four VS preparation pulses with excitation profiles that are spatially shifted by a quarter of the fundamental period of the stripes [20].

Although the recent technical advances made VS preparation quite resistant to  $B_0$  and  $B_1$  field errors, there still remain other non-ideal conditions which may affect the performance of VS preparation. First, the gradient pulses contained in VS excitation are distorted by eddy currents. This distorts excitation profiles over velocity, which may cause signal loss in arterial blood. Second, VS excitation pulses are designed ignoring tissue relaxation and assuming a constant spin velocity. However, practical VS pulse sequences with refocusing are too long to ignore tissue relaxation and accelerated motion. This study aims to investigate the effects of these deviations from the ideal conditions on the performance of VS preparation. Using a double refocused VS preparation pulse as a testbed, we

numerically simulated excitation profiles considering the effects of tissue relaxation ( $T_1$  and  $T_2$ ), eddy currents, and accelerated motion. The resultant decreases in artery-to-muscle contrast are reported for each error source and for their combination.

## 2. Velocity-Selective Preparation Pulse Sequence

Fig. 1A shows a typical FT-VS preparation pulse sequence with paired refocusing, which yields a notch-shaped  $M_z$  response over velocity (Fig. 1B). According to the excitation k-space formalism [2, 21], this pulse sequence deposits RF weights in a form of sampled rectangular function along the  $k_v$ -axis ( $k_v$  is the Fourier variable of velocity  $v$ ), which is Fourier-transformed to transverse magnetization ( $M_{xy}$ ) response of aliased sinc function along velocity. The sinc-shaped  $M_{xy}$  response translates to notch-shaped  $M_z$  response when used for magnetization preparation. The primary design parameters were as follows: flip angle,  $90^\circ$ ; velocity field-of-view (FOV), 60 cm/s; and number of hard RF pulses, 9. A delay period of 0.4 ms was added after each unipolar gradient pulse to reduce eddy current effects. Refocusing pulses were 1.4-ms-long  $90^\circ$ - $180^\circ$ - $90^\circ$  composite pulses and were MLEV-phase-cycled over the sequence. The total pulse duration was 50.6 ms. Note that the  $M_z$ -velocity profile shown in Fig. 1B was simulated assuming no tissue relaxation, no eddy currents, and constant spin velocity. As a result, the  $M_z$  value is zero in the velocity stopband near  $v = 0$  cm/s and  $M_0$  is in the passband ranging from 4.2 cm/s to 55.6 cm/s based on a threshold of  $M_z = 0.8M_0$ . This allows for the maximum possible saturation-based contrast of  $M_0$  between stationary and

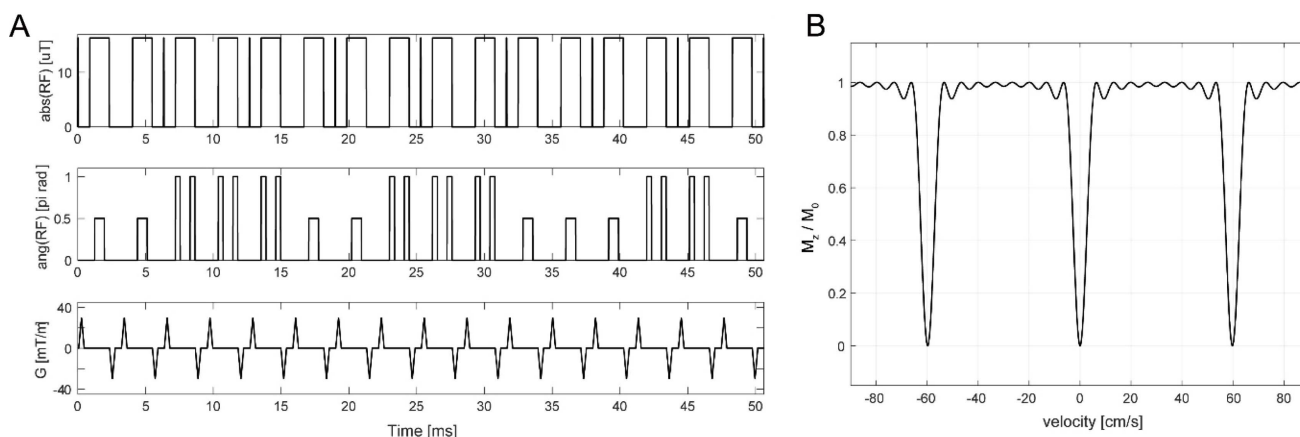


**Fig. 1.** (A) Fourier-transform-based velocity-selective magnetization preparation pulse sequence with paired refocusing. (B) Simulated longitudinal magnetization as a function of spin velocity under assumptions of no relaxation, no eddy current, and constant velocity (*i.e.*, ideal conditions).

moving tissues.

### 3. Numerical Simulations

Bloch-equation-based numerical simulations were performed in MATLAB (MathWorks, Natick, MA, USA) to investigate the effects of non-ideal conditions on the excitation profiles of the testbed FT-VS preparation shown in Fig. 1A. The Bloch equation is written as:

$$\frac{d\mathbf{M}}{dt} = \mathbf{M} \times \gamma \mathbf{B} - \frac{M_x \mathbf{i} + M_y \mathbf{j}}{T_2} - \frac{(M_z - M_0) \mathbf{k}}{T_1} \quad (1)$$

where  $\mathbf{M} = [M_x, M_y, M_z]^T$  is magnetization vector;  $\mathbf{B}$  is net magnetic field resulting from RF and gradient field;  $T_1$  and  $T_2$  represent the time constants for longitudinal and transverse relaxations, respectively. The three non-ideal conditions analyzed were the relaxation times  $T_1$  and  $T_2$ , eddy currents, and accelerated motion. The longitudinal magnetizations of muscle and arterial blood were simulated as representatives of the velocity stopband and passband, respectively. These two  $M_z$  values are supposed to be zero and  $M_0$ , respectively, under ideal conditions. Relative contrast ratio (CR) between arterial blood and muscle tissue signals was calculated as  $(S_A - S_M)/S_A$ , where  $S_A$  and  $S_M$  are the signal intensities of arterial blood and muscle tissue, respectively.

In the analysis of the effects of tissue relaxation, the following relaxation times at a field strength of 3T were used based on the study of Stanisiz *et al.* [22] as follows:  $T_1/T_2 = 1932 \text{ ms}/275 \text{ ms}$  for arterial blood, and  $T_1/T_2 = 812 \text{ ms}/50 \text{ ms}$  for muscle tissue. The muscle tissue was assumed to be stationary (*i.e.*, to have zero velocity), and the arterial blood was assumed to have all the other non-zero velocity values simulated. For the analysis of eddy current effects, the additional gradient waveform generated by eddy currents was simulated using the approximation model based on convolutions with exponential decay as described previously [23, 24].

$$G_{\text{eddy}}(t) = -\frac{dG(t)}{dt} * Ae^{-\frac{t}{\tau}} \quad (2)$$

where  $G(t)$  and  $G_{\text{eddy}}(t)$  represent the original gradient and additional gradient due to eddy currents, respectively;  $A$  and  $\tau$  represent the amplitude and time constant of eddy current. The simulation was performed for spins at spatial offsets of  $[-20, +20]$  cm from the iso-center, with the eddy current amplitude of 0.25 %, and time constant ranging from 0.1 to 1000 ms. Two spin velocities of 0 cm/s and 26.5 cm/s were selected as representative values for the velocity stopband and passband, respectively. Note

that the passband velocity of 26.5 cm/s was purposely chosen as it yields exactly  $M_z = M_0$ , while the  $M_z$  response exhibits a small degree of fluctuation in the velocity passband due to the Gibbs ringing induced by rectangular k-space weighting. A post-gradient delay of 0.4 ms or 0.02 ms was used for the simulation to investigate its effect on eddy current effects.

To estimate a proper range of acceleration to be simulated, phase contrast (PC) flow measurements of arterial blood obtained in an earlier study were used [7]. The PC data were obtained in the bilateral popliteal arteries of 31 patients with peripheral artery disease. For each time-velocity curve obtained from 62 arterial regions of interest (ROIs), the acceleration or deceleration value was computed by linear fitting of the curve during velocity increase or decrease before or after the peak systolic cardiac phase. A mean acceleration of 325 cm/s<sup>2</sup> and a mean deceleration of 174 cm/s<sup>2</sup> obtained from the analysis were used in the simulation. Note that these two values are practically the maximum deviations from constant velocity assuming the cardiac trigger delay for VS preparation is synchronized close to the peak systole. Finally, combinations of tissue relaxation, eddy currents, and acceleration were simulated to investigate their net effect on the performance of VS preparation. The relative CR between arterial blood and muscle tissue was simulated for varying eddy current conditions. Arterial blood was assumed to have a velocity of 26.5 cm/s as in the eddy-current-only simulation and an acceleration of 325 cm/s<sup>2</sup> as in the acceleration-only simulation.

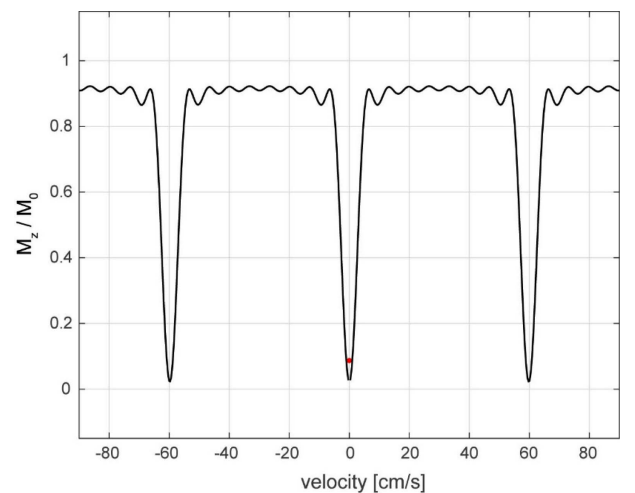


**Fig. 2.** Longitudinal magnetization ( $M_z$ ) resulting from the VS excitation pulse shown in Fig. 1A over velocity with consideration of tissue relaxation.  $M_z$  responses of muscle and arterial blood are denoted by the red circle and black line, respectively.

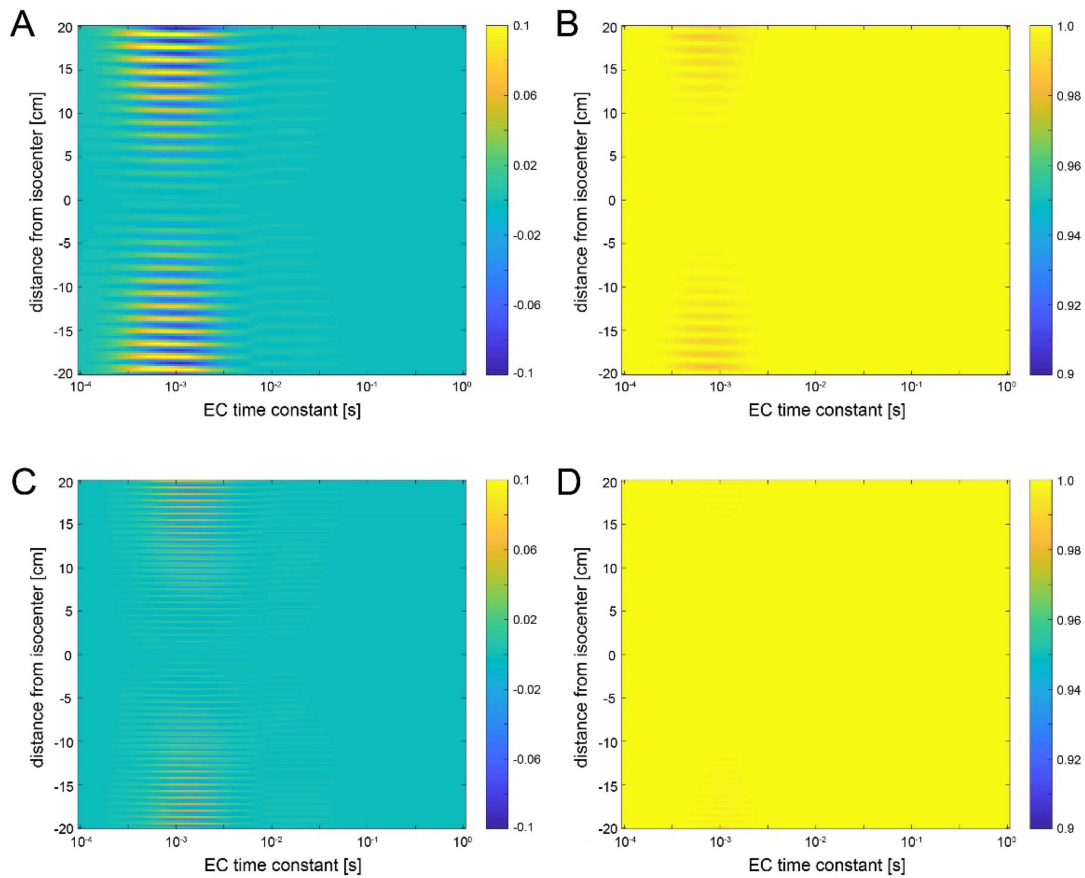
## 4. Results

Figure 2 shows the  $M_z$ -velocity response simulated considering the  $T_1$  and  $T_2$  values of muscle with zero velocity (denoted by red circle) and arterial blood with non-zero velocities (black line). Muscle  $M_z$  increased from the ideal value of zero to  $0.09M_0$ , and arterial blood  $M_z$  decreased from the ideal value of  $M_0$  to  $0.92M_0$ . These arterial and muscle  $M_z$  values amount to a relative CR of 0.90, which is smaller than the ideal CR of 1.0 by 10 %.

Figure 3 shows the effects of eddy currents on the longitudinal magnetizations of muscle (Fig. 3A, C) and arterial blood (Fig. 3B, D), which were assumed to have the velocities of 0 cm/s and 26.5 cm/s, respectively. When the minimal delay of 0.02 ms was added after every gradient pulse, VS preparation yielded significant fluctuation in muscle  $M_z$  (Fig. 3A) and a marginal decrease in arterial blood  $M_z$  (Fig. 3B), especially at large spatial offsets from the iso-center. Within the considered ranges of off-center distance and eddy current time constant, the maximum

muscle  $M_z$  and the minimum blood  $M_z$  were  $0.11M_0$  and  $0.98M_0$ , respectively, which translate to the worst case relative CR of 0.89. When a post-gradient delay of 0.4 ms was applied, the eddy-current-induced error significantly decreased in both muscle and arterial blood magnetizations (Fig. 3C-D). The maximum muscle  $M_z$  and the minimum blood  $M_z$  were  $0.05M_0$  and  $0.99M_0$ , respectively, corresponding to the worst case relative CR of 0.95. This would be a negligible loss of image contrast in angiography applications (only by 5 % relative to the ideal CR).

According to the analysis of PC flow data, the acceleration of arterial flow before and after the peak systole were  $325.2 \pm 157.4$  cm/s<sup>2</sup> and  $-173.8 \pm 89.6$  cm/s<sup>2</sup>, respectively. Representative time-velocity curves and the resultant linear fits for the estimation of acceleration are shown in Fig. 4A. Fig. 4B shows  $M_z$  response versus mean velocity when the spins move with a constant acceleration of 325 cm/s<sup>2</sup> (blue) or  $-174$  cm/s<sup>2</sup> (red). Only velocity-passbands were considered for the simulation since these two acceleration values were measured for



**Fig. 3.** (Color online) (A-B) Effect of eddy currents on longitudinal magnetization of (A) a stationary spin and (B) a spin with velocity of 26.5 cm/s when 0.02 ms-long delay is used after every gradient pulse in VS preparation pulse sequence. (C-D) Effect of eddy currents when 0.4 ms-long delay is used after every gradient pulse.

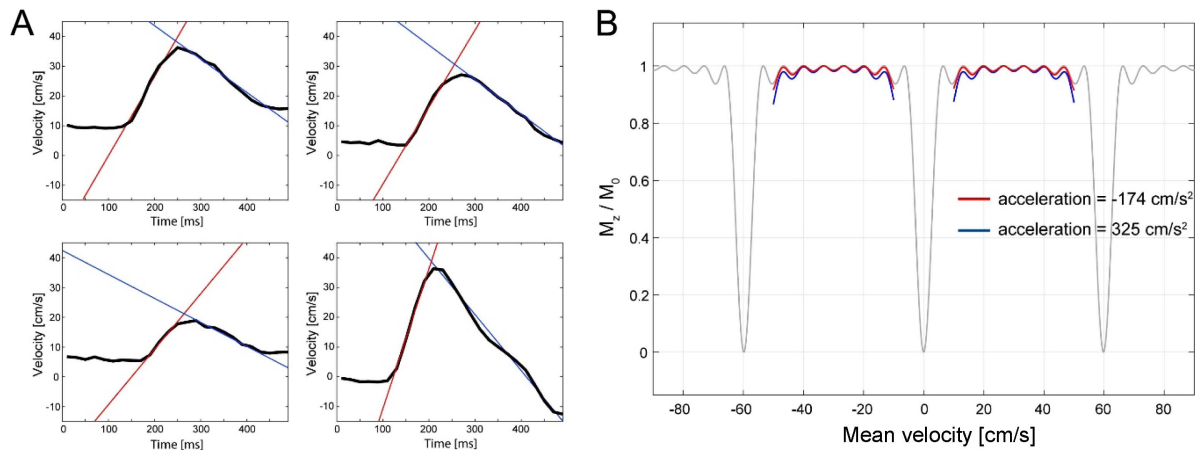


**Fig. 4.** (Color online) (A) Representative time-velocity curves measured in the popliteal arteries of four subjects, and linear fitting of the curve during velocity increase (red line) or decrease (blue line) for the estimation of acceleration or deceleration. (B) Longitudinal magnetization profile versus mean velocity when spins are moving with a constant acceleration of  $325 \text{ cm/s}^2$  (blue) or a constant deceleration of  $174 \text{ cm/s}^2$  (red).

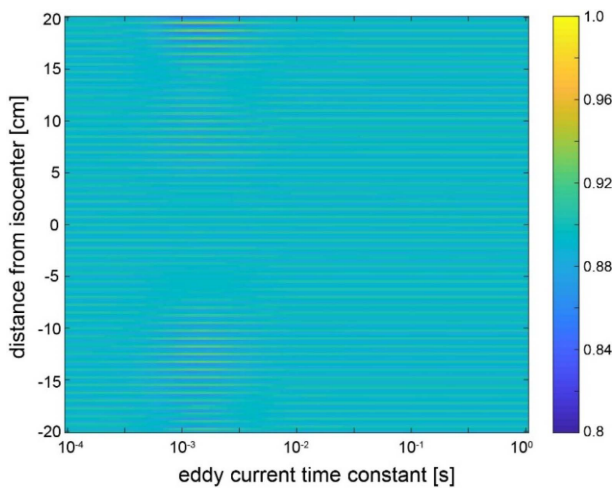


**Fig. 5.** (Color online) Simulated relative contrast ratio between stationary muscle and arterial blood with a mean velocity of  $26.5 \text{ cm/s}$  and an acceleration of  $325 \text{ cm/s}^2$  under consideration of tissue relaxation and varying eddy current conditions. The minimum relative contrast ratio was found to be 0.86.

velocities sufficiently higher than the cutoff velocity ( $4.2 \text{ cm/s}$ ). For the deceleration of  $174 \text{ cm/s}^2$ , the  $M_z$  profile barely deviated from the reference profile obtained with no acceleration (grey). For the acceleration of  $325 \text{ cm/s}^2$ , the  $M_z$  profile got slightly blurred near the lower and upper bounds of the velocity passband, indicating that acceleration reduces the magnetization of slowly moving arterial blood to only a marginal degree. The lowest (the worst-case) arterial blood  $M_z$  for the simulated velocity range was  $0.88 M_0$ . Figure 5 shows the simulated relative CR between muscle tissue and arterial blood (with an

assumed velocity of  $26.5 \text{ cm/s}$  and an acceleration of  $325 \text{ cm/s}^2$ ) under consideration of tissue relaxation and varying eddy current conditions. The minimum CR was found to be 0.86 which translates to a loss of CR by 14 % relative to the ideal value of 1.0.

## 5. Discussion

In this study, we investigated the effects of tissue relaxation, eddy currents, and accelerated motion on FT-VS preparation pulses, which are often ignored during the pulse design. Arterial blood  $M_z$  resulting from FT-VS preparation turned out to decrease from the ideal value of  $M_0$  to  $0.92M_0$ ,  $0.99M_0$ , and  $0.88M_0$  due to the effects of tissue relaxation, eddy currents, and accelerated motion, respectively. When all three factors were considered simultaneously, the worst-case relative CR between arterial blood and muscle was estimated as 0.86.

While the effect of tissue relaxation can be represented by fixed  $M_z$  values for arterial blood ( $0.91M_0$ ) and muscle tissue ( $0.09M_0$ ), the effects of eddy currents and acceleration are quite variable depending on the values of related imaging and MR system parameters. The eddy current effect was large for limited ranges of off-isocenter distance ( $> 5 \text{ cm}$ ) and eddy current time constant (around  $10^{-3} \text{ sec}$ ) when a minimal post-gradient-delay ( $0.02 \text{ ms}$ ) was used. This trend was maintained when a post-gradient-delay of  $0.4 \text{ ms}$  was used, but the severity of excitation error was substantially reduced as verified by negligible worst-case loss in relative blood-to-muscle contrast ( $0.06M_0$ ). The effectiveness of marginal delay of  $0.4 \text{ ms}$  is presumably due to small size of preceding

gradient pulses ( $\sim 0.4$  ms).

The effect of accelerated motion is closely related to the cardiac trigger delay (TD) which determines the timing for applying VS preparation pulses. When the TD is ideally set to the peak systolic phase, arterial flow velocity would be nearly constant during the VS preparation ( $\sim 50$  ms). Scout PC flow measurements can find the ideal value of TD but need extra time for scan and analysis. The use of pre-defined TD values is more practical (*e.g.*, the average of ideal values obtained in a group of subjects) but more likely to involve accelerated motion during the VS preparation due to deviations from the peak systole. The acceleration values of  $325 \text{ cm/s}^2$  and  $-174 \text{ cm/s}^2$  used in our simulation were obtained from monotonically increasing or decreasing parts of time-velocity curves (refer to examples in Fig. 4A) and correspond to a significant deviation of TD from the peak flow phase. Nevertheless, the resultant  $M_z$  profile showed marginal blurring only near the lower bound of the velocity passband. This will slightly reduce signals originating from slow-moving arterial blood but will not affect those obtained from arterial blood with moderate-to-high velocity.

There are limitations of directly translating the results of numerical simulations to in-vivo cases. First, the numerical simulation combined the worst-case effects of tissue relaxation, eddy currents, and acceleration. The effect of relaxation is deterministic, but the effects of eddy currents and acceleration vary significantly depending on imaging and system parameters. The actual contributions of these two factors are likely smaller than the values indicated by the numerical simulation representing the worst-case combination. Conversely, our numerical simulations did not consider  $B_0$  and  $B_1$  field errors which have already been reported in several earlier studies [2-4, 7, 15]. With the double refocused design used in this study, the signal of arterial blood in the velocity passband is not prone to the effects related to  $B_0$  and  $B_1$  field offset. However, the signal of stationary tissues in the stopband varies depending on actual  $B_1$  strength, which is partially responsible for the decrease of relative CR from the ideal value. Finally, in-vivo blood-to-muscle contrast would vary among subjects, depending on the pattern of arterial blood flow and the MR system used. In particular, the longitudinal magnetization at equilibrium ( $M_0$ ) itself varies depending on RF heating and MR room temperature, which is not accounted for in this study.

## 6. Conclusion

The longitudinal magnetization of arterial blood resulting from a FT-VS preparation pulse decreases from the ideal

value of  $M_0$  to  $0.92M_0$ ,  $0.99M_0$ , and  $0.88M_0$  due to tissue relaxation, eddy currents, and accelerated motion, respectively. When all three factors are considered simultaneously, the worst-case relative contrast ratio between arterial blood and muscle tissue is estimated as 0.86, corresponding to a decrease by 14 % from the ideal contrast ratio of 1.0.

## Acknowledgements

This work was supported by the National Research Foundation of Korea funded by the Ministry of Science and ICT (NRF-2020R1A2C1006293) and the Ministry of Education (NRF-2020R1A6A1A03043528), and by Institute of Information & communications Technology Planning & Evaluation (IITP) grant funded by the Korea government (MSIT) (No. RS-2022-00155966, Artificial Intelligence Convergence Innovation Human Resources Development [Ewha Womans University]).

## References

- [1] L. de Rochefort, X. Maître, J. Bittoun, and E. Durand, *Magn. Reson. Med.* **55**, 171 (2006).
- [2] Z. Zun and T. Shin, *NMR Biomed.* e4820 (2022).
- [3] T. Shin, P. W. Worters, B. S. Hu, and D. G. Nishimura, *Magn. Reson. Med.* **69**, 1268 (2013).
- [4] T. Shin, B. S. Hu, and D. G. Nishimura, *Magn. Reson. Med.* **70**, 1229 (2013).
- [5] Q. Qin, T. Shin, M. Schar, H. Guo, H. Chen, and Y. Qiao, *Magn. Reson. Med.* **75**, 1232 (2016).
- [6] T. Shin, *Invest. MRI* **25**, 209 (2021).
- [7] T. Shin, R. G. Menon, R. B. Thomas, A. U. Cavallo, R. Sarkar, R. S. Crawford, and S. Rajagopalan, *J. Magn. Reson. Imaging* **49**, 744 (2019).
- [8] W. Li, F. Xu, M. Schär, J. Liu, T. Shin, Y. Zhao, P. C. M. van Zijl, B. A. Wasserman, Y. Qiao, and Q. Qin, *Magn. Reson. Med.* **79**, 2014 (2018).
- [9] D. Zhu, W. Li, D. Liu, G. Liu, F. Sadaghat, Y. Pei, T. Shin, and Q. Qin, *Magn. Reson. Med.* **83**, 1173 (2020).
- [10] D. B. Watson, B. Grasu, R. Menon, R. Pensy, R. S. Crawford, and T. Shin, *J. Vasc. Surg. Cases & Innov. Tech.* **3**, 87 (2017).
- [11] Q. Qin and P. C. M. van Zijl, *Magn. Reson. Med.* **74**, 1136 (2016).
- [12] D. Liu, F. Xu, W. Li, P. C. M. van Zijl, D. D. Lin, and Q. Qin, *Magn. Reson. Med.* **84**, 2512 (2020).
- [13] V. Landes, A. Javed, T. Jao, Q. Qin, and K. S. Nayak, *Magn. Reson. Med.* **84**, 1909 (2020).
- [14] Q. Qin, et al. *Magn. Reson. Med.* **88**, 1528 (2022).
- [15] J. Guo, S. Das, and L. Hernandez-Garcia, *Magn. Reson. Med.* **85**, 2027 (2021).
- [16] T. Shin, Q. Qin, J.-Y. Park, R. S. Crawford, and S. Raja-

- gopalan, *Magn. Reson. Med.* **76**, 466 (2016).
- [17] M. H. Levitt and R. Freeman, *J. Magn. Reson.* **33**, 473 (1979).
- [18] M. Levitt, R. Freeman, and T. Frenkiel, *J. Magn. Reson.* **47**, 328 (1982).
- [19] A. J. Shaka, S. P. Ruckert, and A. Pines, *J. Magn. Reson.* **77**, 606 (1988).
- [20] T. Shin and Q. Qin, *Magn. Reson. Med.* **80**, 1997 (2018).
- [21] J. Pauly, D. G. Nishimura, and A. Macovski, *J. Magn. Reson.* **81**, 43 (1989).
- [22] G. J. Stanisz, E. E. Odobina, J. Pun, M. Escaravage, S. J. Graham, M. J. Bronskill, and R. M. Henkelman, *Magn. Reson. Med.* **54**, 507 (2005).
- [23] J. J. V. Vaals and A. H. Bergman, *J. Magn. Reson.* **90**, 52 (1990).
- [24] J. A. Meakin and P. Jezzard, *Magn. Reson. Med.* **69**, 832 (2013).